J Math Chem (2009) 46:952–961
DOI 10.1007/s10910-009-9556-y

ORIGINAL PAPER

Optical properties of ultra small Si nanoparticles: potential role of surface reconstruction and oxygen contamination

C. S. Garoufalis · A. D. Zdetsis

Received: 6 September 2006 / Accepted: 30 September 2008 / Published online: 14 July 2009

Abstract We report accurate high level calculations of the optical gap and absorption spectrum of ultra small Si nanocrystals, with hydrogen and oxygen passivation, (with and without surface reconstruction). Our calculations have been performed in the framework of time dependent density functional theory (TDDFT) using the hybrid nonlocal exchange and correlation functional of Becke and Lee, Yang and Parr (B3LYP) and the multireference second-order perturbation theory (MR-MP2). We show that some of the details of the absorption and emission properties of the 1 nm Si nanoparticles can be efficiently described in the framework of TDDFT/B3LYP, by considering the effect of surface reconstruction and the geometry relaxation of the excited state. Additionally, we have examined the effect of oxygen contamination on the optical properties of 1 nm nanoparticles and its possible contribution to their experimentally observed absorption and emission properties.

Keywords Silicon nanocrystal · Oxygen passivation · Optical properties · Surface reconstruction

1 Introduction

The visible photoluminescence of porous silicon (p-Si) and silicon nanoparticles has attracted a lot of attention in recent years, both experimentally and theoretically [1–19]. A large portion of this work has been devoted to understanding the visible photoluminescence of Si nanocrystals and correlating its spectrum with the diameter of the nanoparticles.

C. S. Garoufalis · A. D. Zdetsis (✉)
Department of Physics, University of Patras, 26500 Patras, Greece
e-mail: zdetsis@upatras.gr

The majority of the earlier experimental work led to diverse results as for the size of the Si dots capable of emitting in the visible. Some of the initial discrepancies could be resolved by considering the impact of surface oxidation on the optical properties of the nanocrystals. In particular, it was found that the surface oxygen atoms (especially the Si=O bonding) can reduce significantly the optical gap of such nanostructures and make visible light emission possible even for nanoparticles with diameters below 15 Å [8–16].

However, there are recent experimental data [17] which report the detection of luminescent ultra small hydrogen passivated Si nanoparticles, with diameters in the range of 1 nm. The size of the particles was determined by direct high-resolution TEM imaging, while infrared and electron photospectroscopy showed that they were highly passivated with hydrogen. In this diameter range, there are two candidate nanoclusters (Si_{29} and Si_{35}) which may be considered responsible for the observed absorption and emission spectra. The reported absorption peak at 3.5 eV is found to be in clear contrast to existing theoretical predictions concerning the $Si_{29}H_{36}$ nanocrystal. In particular, there are accurate calculations based on the sophisticated MR-MP2 method, which predict an optical gap of 4.45 eV for the $Si_{29}H_{36}$ cluster [6].

This discrepancy led several researchers to consider that the obvious disagreement between experiment and theory could be resolved either by examining the possible surface reconstruction patterns of the Si_{29} nanoparticle [18,19], or the effect of oxygen contamination.

Since the accuracy and suitability of a computational approach cannot be taken for granted, it is common practice to validate the reliability of the theoretical calculations by comparing their results either with existing experimental data, or with the results of more advanced and sophisticated calculations. However, the direct comparison with experiment may sometimes be misleading. This can be easily understood if we consider that theoretical calculations are always performed on well established and controllable condition (e.g. the structure, composition and environment are well determined), while this is not the case in real world. As a result, the choice of a theoretical approximation (which is compromise between computational cost and rigor) should always be thoroughly investigated. It is clear therefore that, high level accurate ab initio theoretical methods, which can produce unbiased and realistic results, should be used when possible.

With this aim, we present in this work accurate calculations of the optical gap and the optical absorption spectrum of ultra small Si nanoparticles, based on time-dependent density functional theory [20] using a hybrid and a non hybrid functional (B3LYP [21] and BP86 [22,23]) and the high level multireference second-order perturbation theory (MR-MP2) [24,25]. The later is used, mostly, as a reliable method, which can validate the accuracy of TDDFT/B3LYP and TDDFT/BP86 results.

2 Outline of calculations

The nanoparticle considered in this work, are the fully hydrogenated $Si_{29}H_{36}$ and $Si_{35}H_{36}$, the 2×1 reconstructed $Si_{29}H_{24}$ and several oxygen contaminated variants

of the $Si_{29}H_{36}$ and $Si_{35}H_{36}$ nanoparticles. In all cases the geometries have been fully optimized in a DFT/B3LYP level of theory.

All DFT and the TDDFT calculations were performed with the TURBOMOLE [26] suite of programs using Gaussian atomic orbital basis sets of split valence [SV(P)]: [4s3p1d]/2s [27] quality. The TDDFT calculations have been performed as described in detail in Refs. [6,28] using the B3LYP functional consistently for both, the self-consistent solution of the Kohn–Sham equation for the ground state, and the solution of the linear response problem. The MR-MP2 calculations were performed as described in Ref. [29]. As we have shown elsewhere [6], the partially exact Hartree–Fock (HF) exchange that is included in the B3LYP method is crucial for the correct description of the optical properties. We have verified this by performing additional TDDFT calculations using the well known functional of Becke and Perdew (BP86) [22,23], which does not include exact (or partially exact) exchange. The (partially) exact Hartree–Fock (HF) exchange seems to be especially important for small size nanocrystals. Furthermore, the inclusion of exact HF exchange remedies the well-known deficiency of local-density approximation (LDA) to underestimate the band gap.

3 Results and discussion

3.1 Surface reconstruction

The first step in the calculation of the optical properties of $Si_{29}H_{24}$ reconstructed nanoparticle was to study the energetics of the mechanism, through which, the surface reconstruction can take place. This information is considered important, since it can give us an insight on the relative stability of the reconstructed nanocluster. In particular we have calculated the energy barrier of the reaction $Si_{29}H_{34} + H_2 \leftrightarrow Si_{29}H_{36}$. In order to model any reaction, it is necessary to find the transition structure which connects the products with the reactants. For the specific case, the transition structure was obtained using the quadratic synchronous transit approach (QST2) implemented in the Gaussian03 program [30]. These calculations were performed without any symmetry constrain, using the semiempirical AM1 approximation. The same transition structure was also implied by selective DFT potential energy surface scans. The energy differences shown in Fig. 1 are derived by DFT/B3LYP calculations on the AM1 geometries. As it can be seen in Fig. 1, we find a significant energy barrier separating the two PES minima ($Si_{29}H_{36}$ and $Si_{29}H_{34}$). This implies that both structures can be stable, while the existence of either of them depends on the experimental procedure.

In order to examine if the experimentally observed [17] absorption peaks (3.7, 4.0 and 4.6 eV) of these nanoparticles can be truly explained by means of surface reconstruction, we have calculated the TDDFT optical absorption spectrum of the $Si_{29}H_{24}$ (reconstructed cluster) using both the hybrid B3LYP and non-hybrid BP86 functionals. The performance of the two functional, for the case of Si nanocrystals, has been tested elsewhere [6], revealing that B3LYP produces accurate excitation energies, while BP86 exhibits a systematic underestimation of approximately 0.6 eV. Despite the fact that BP86 includes gradient corrections, its results are in general agreement with the corresponding TDLDA.

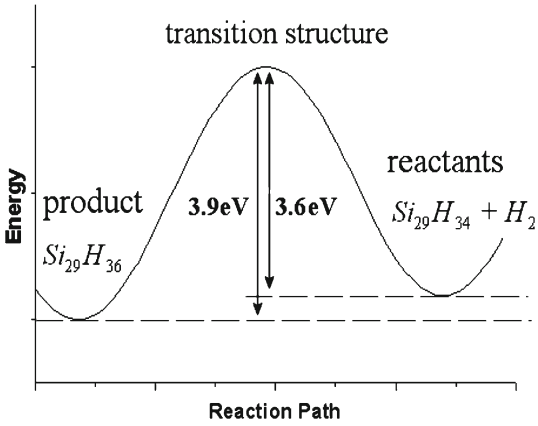

Fig. 1 Potential energy surface of the reaction $Si_{29}H_{34} + H_2 \leftrightarrow Si_{29}H_{36}$

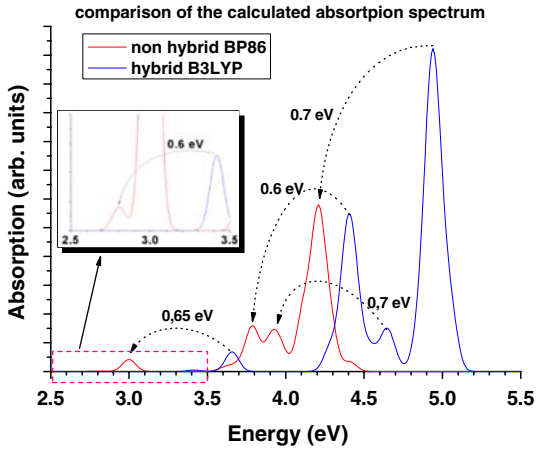

Fig. 2 Calculated optical absorption spectrum of the $Si_{29}H_{24}$ nanoparticle

The calculated (TDDFT/B3LYP and TDDFT/BP86) absorption spectrum of $Si_{29}H_{24}$ clusters is shown in Fig. 2. The first thing that can be observed in this figure is that the TDDFT results of the non-hybrid BP86 functional are systematically 0.6–0.7 eV lower than the corresponding of the B3LYP. The same systematic trend has also been observed in earlier calculations. By closer inspection, we can see that the TDDFT/BP86 the absorption threshold is approximately 2.8–3.0 eV. The rest of the most prominent excitation energies are at 3.6, 3.8, 3.9 and 4.2 eV. Since the calculation was limited to the 20 lowest spin and symmetry allowed transition, there are no available data for lager energies. If the absorption threshold of 2.8 eV is neglected or "wrongly" associated with the experimentally observed weak emission peak at 2.8 eV, then the rest of the calculated (TDDFT/BP86) spectrum seems to be in a reasonable agreement with the experimental data. However, since for Si nanocrystals the emitted radiation exhibits a significant Stokes shift (tenths of eV), the absorption peak at 2.8 eV should produce an emission peak of ∼2.3 eV. As a result, it becomes clear that either the non-hybrid BP86 functional fails to predict the details of the experiment, or the observed peaks cannot be attributed to the $Si_{29}H_{24}$ nanoparticle.

The results of TDDFT/B3LYP calculations give a completely different perspective. The lowest (and weakest) peak is located at 3.4 eV while the rest of them are located at 3.65, 4.4, 4.65 and 4.95 eV, systematically blueshifted by 0.6–0.7 eV compared to the corresponding TDDFT/BP86 results. The first peak at 3.4 eV corresponds to the HOMO-LUMO transition, while the second one is a mixture of the HOMO-2 $\rightarrow$ LUMO (63%) and HOMO-1 $\rightarrow$ LUMO (35%) transitions. Since the first peak is almost vanishing, the actual absorption threshold can be considered to correspond to the second one, which is in excellent agreement with the experimental value of 3.7 eV. The calculated small absorption at 3.4 eV can be associated with the experimental weak emission at 2.8 eV if the Stokes shift is taken into account. For these reasons we have performed an additional geometry optimization of the lowest excited state using again the TDDFT/B3LYP methodology. For this type of calculation, it is necessary to lower the symmetry of the nanoparticle in order to give it the flexibility required for the geometry relaxation of the excited state. At this point, motivated by a recent paper by Sundholm [31], who has performed similar calculations on the $Si_{29}H_{36}$ nanoparticle and concluded that the symmetry of the first excited state is D2d, we further lower the symmetry of our $Si_{29}H_{24}$ cluster to D_2 (subgroup of the initial Td symmetry). For the completely relaxed geometry we find the emission energy to be 2.9 eV (a Stokes shift of 0.5 eV) in very good agreement with the experimentally observed emission peak of 2.8 eV. Moreover, the calculated Stoke shift of 0.5 eV is in excellent agreement with the experimental values of 0.51, 0.56 and 0.53 eV. As a result the experimentally observed weak emission peak can be readily attributed to the lowest allowed absorption peak at 3.4 eV. At this point, it should be noted that selective test calculations with the sophisticated MR-MP2 method [24,25] reveal a remarkable agreement of the MR-MP2 lowest allowed excitation energies (within 0.2 eV) with the results of TDDFT/B3LYP calculations validating the accuracy and efficiency of the B3LYP functional. In particular, for the case of $Si_{29}H_{24}$ nanoparticle the MR-MP2 lowest allowed electronic transition is found to be 3.6 eV. This value is in very good agreement with the 3.4 eV of TDDFT/B3LYP and the 3.5 eV of recent QMC calculations [18] and validates the accuracy and efficiency of the B3LYP functional. On the other hand it is now well established that the TDDFT calculation with a non-hybrid functional (in this case BP86) systematically underestimates the excitation energies nanocrystals by as much as 0.6 eV.

However, despite the excellent agreement of calculated and experimental absorption (and emission) thresholds achieved thus far, a problem arises with the experimentally observed absorption peak at 4.0 eV. As it can be seen in Fig. 2, the calculation fails to predict any absorption in the energy region between 3.7 and 4.3 eV.

As it becomes evident from the above discussion, both theoretical calculations (TDDFT/BP86 and TDDFT/B3LYP) fail to reproduce some aspects of the experimental data. As a result, it seems reasonable to pursue alternative (or complementary) to surface reconstruction interpretation. The first possibility that comes into mind is that there might be contributions from Si_{29} nanoparticles which are subdued only to a partial surface reconstruction. However, TDDFT calculations on the $Si_{29}H_{34}$ nanoparticle (Fig. 3) revealed that this is not the case.

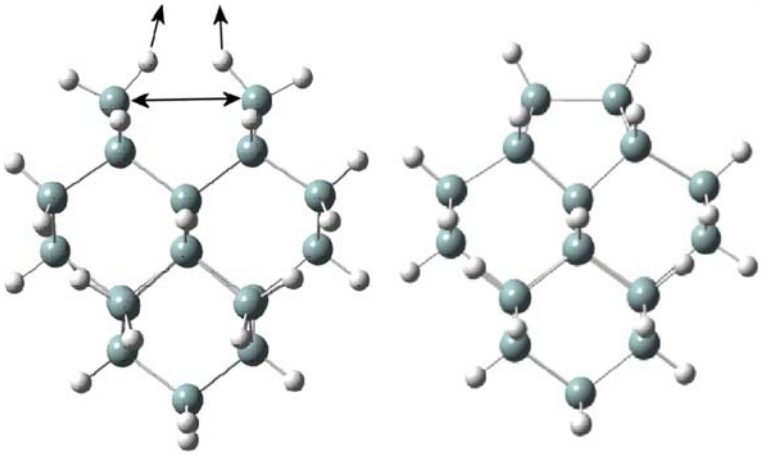

Fig. 3 Surface reconstruction

A second possibility is that, due to size dispersion, there might be contributions from slightly larger nanoparticles. However, a simple examination of the excitation energies of $Si_{35}H_{36}$ nanocrystal reveals that there is no absorption at 4.0 eV.

In this context it seems reasonable to consider the possibility that the observed characteristics of the absorption and emission spectrum of the 1 nm nanoparticles are due to contribution from different species. For example there might be oxygen contaminated nanocrystals (with Si=O or Si–O–Si bonds) which are responsible for some of the experimentally observed optical properties.

3.2 Oxygen contamination

Besides the effect of surface reconstruction and in particular the potential role of the $Si_{29}H_{24}$ nanocluster to the experimentally observed optical properties of 1 nm nanoparticles, we have also examined the possible role of oxygen contamination. As stated by Akcakir et al. [17], the process they adopted for the production of their samples led to nanoparticles which were highly passivated by hydrogen. However, as mentioned by Rao et al. [19], although they consider oxygen contamination less probable, the presence of surface oxygen atoms cannot be completely excluded. For this reason they draw their conclusion (about the absence of oxygen) based on the existing literature on oxygen passivated nanocrystals.

In the next paragraphs it will be shown that the general characteristics 1 nm Si nanoparticles absorption spectrum are, in practice, also consistent with the hypothesis of oxygen contamination. For this reason we have considered several oxygen contaminated variants of the unreconstructed $Si_{29}H_{36}$ nanoparticle. As it has been shown elsewhere [6] by MR-MP2 calculation, the optical gap of $Si_{29}H_{36}$ cluster is 4.45 eV and as a result the experimentally observed optical properties cannot be attributed to this nanoparticle. However, if only a few Si=O double bonds are considered, then the optical properties of these nanoparticles changes dramatically [15]. In Fig. 4 we

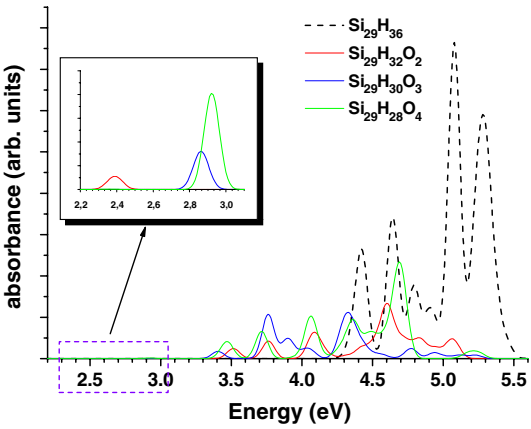

Fig. 4 TDDFT/B3LYP absorption spectrum

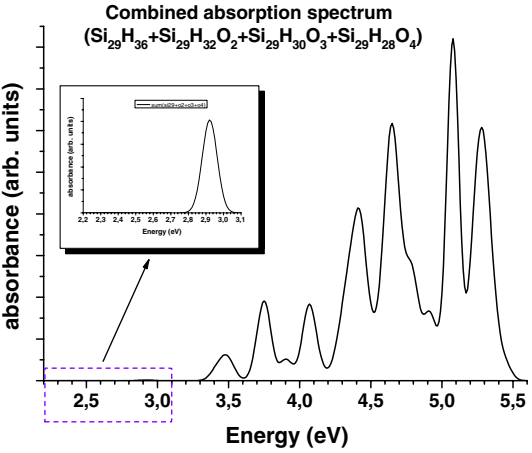

Fig. 5 Calculated absorption spectrum derived by summing up the contributions of the $Si_{29}H_{36}$, $Si_{29}H_{34}O_1$, $Si_{29}H_{32}O_2$, $Si_{29}H_{30}O_3$ and $Si_{29}H_{28}O_4$ nanoparticles

have plotted the absorption spectrum of $Si_{29}H_{36}$, $Si_{29}H_{34}O_1$, $Si_{29}H_{32}O_2$, $Si_{29}H_{30}O_3$ and $Si_{29}H_{28}O_4$, which exhibits many similarities with the experimentally observed from the 1 nm nanoparticles. We can see that the oxygenated clusters exhibit absorption peaks around 3.5 eV as was expected by the experiment. Additionally, by closer inspection we can also see very weak (almost vanishing) peaks around 2.8 eV. Since these peaks are almost vanishing, the actual absorption threshold can be considered to correspond to the peaks located around 3.5 eV. This value is in very good agreement with the experiment.

If we assume that in a colloid suspension as the one reported by Akcakir et al. [17] the aforementioned variants of Si_{29} nanoparticle may coexist, then by summing up their contribution we can plot the absorption spectrum of Fig. 5. In this case, besides the good agreement between calculated and experimental absorption thresholds, we also see the previously missing (for surface reconstructed clusters) peak around 4.0 eV.

Although these results seem to be rather encouraging, the hypothesis of oxygen contamination (via Si=O bonds) appears to be problematic when considering

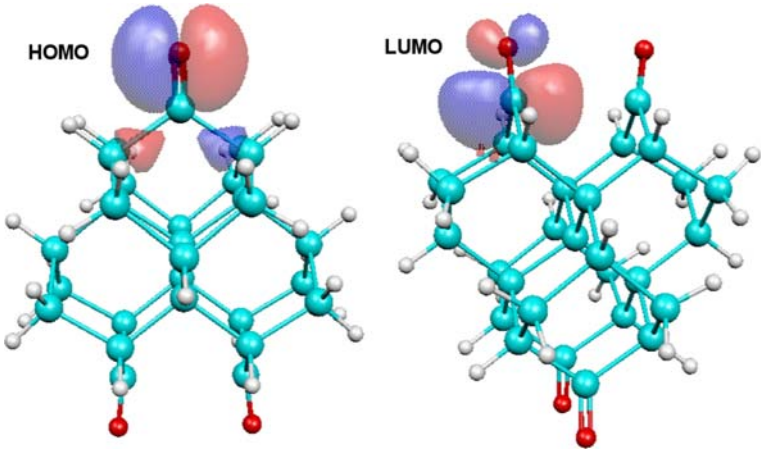

Fig. 6 The HOMO and LUMO natural bond orbitals of $Si_{29}H_{28}O_4$ nanoparticle. It is evident that these orbitals are spatially localized around oxygen sites

the emission properties of these nanoparticles. It is found that the presence of doubly-bonded oxygen affects mainly the tail of the conduction band by inserting new oxygen related states. A natural bond analysis reveals that the HOMO orbital corresponds to Si=O π bonding state, while the LUMO orbital corresponds to the π^* antibonding state (Fig. 6). As a result, all the excited states which include significant contribution from the LUMO orbital (and maybe LUMO+1…) may exhibit large Stokes shifts due to structural relaxation. This is facilitated by the fact that the excitation to the π^* antibonding state transforms the Si=O double bond to a single Si–O bond. As a result the main contribution to the structural relaxation comes from a simple elongation of the Si–O bond. In this case, the Stokes shift between absorption and emission can be even larger than 1.0 eV, making the calculated emission spectrum to be inconsistent with the experiment.

Oxygen contamination can also take place through the formation of surface Si–O–Si bridging bonds. In this case, the calculated absorption thresholds are found to depend on the number of surface oxygen atoms. For example, the TDDFT/B3LYP fundamental optical gap for $Si_{29}H_{34}O$ and $Si_{29}H_{24}O_6$ oxygen contaminated nanoparticles is found to be 4.1 and 3.6 eV, respectively. As a result the agreement between calculated and experimental absorption thresholds depends on the number of oxygen contaminants. For these nanoparticles the smaller Stoke shift (compared to Si=O) makes the emission spectrum more consistent with the experiment.

From the above discussion, it becomes evident that both the effects of surface reconstruction and oxygen contamination offer some attractive explanations for specific features of the experimental data, while on the same time they also exhibit some problematic aspects.

4 Conclusions

In conclusion, we have studied the effect of surface reconstruction and oxygen contamination on the optical properties of 1 nm Si nanoparticles (Si_{29}) using three different

theoretical techniques. It is shown that (1) the TDDFT/B3LYP excitation energies are found to be in good agreement with the results of high level MR-MP2 calculations and, at least for the case of Si nanocrystals, they can be trusted. (2) the TDDFT/BP86 calculated absorption spectrum is systematically redshifted by as much as 0.6–0.7 eV compared to the TDDFT/B3LYP. This underestimation is most likely due to its no-hybrid nature and it may also be true for other non-hybrid functionals (and LDA calculations). (3) The experimentally observed absorption and emission thresholds of 1 nm nanoparticles are consistent with the hypothesis of surface reconstruction and they are successfully described in the framework of TDDFT/B3LYP. However these calculations fail to produce some of the experimental details. (4) Oxygen contamination through surface Si=O and Si–O–Si species can significantly affect the optical properties of 1 nm nanoparticles. For the case of Si=O bonds the results are consistent with the experimental data as far as it concerns absorption, but due to large Stokes shifts (>1 eV) fail to reproduce the experimental emission data. When oxygen contamination occurs through Si–O–Si bonds, the absorption thresholds exhibit a significant dependence on the amount of oxygen while, due to smaller Stoke Shift, the emission properties of the nanoparticles are in better agreement with experiment.

Acknowledgments We thank the European Social Fund (ESF), Operational Program for Educational and Vocational Training II (EPEAEK II), and particularly the Program PYTHAGORAS, for funding the above work.

References

1. L.T. Canham, Appl. Phys. Lett. **57**, 1046 (1990)
2. J.P. Wilcoxon, G.A. Samara, P.N. Provencio, Phys. Rev. B **60**, 2704 (1999)
3. M.V. Wolkin, J. Jorne, P.M. Fauchet, G. Allan, C. Delerue, Phys. Rev. Lett. **82**, 197 (1999)
4. S. Schuppler, S.L. Friedman, M.A. Marcus, D.L. Adler, Y.H. Xie, F.M. Ross, Y.L. Cha-bal, T.D. Harris, L.E. Brus, W.L. Brown, E.E. Chaban, P.F. Szajowski, S.B. Christman, P.H. Citrin, Phys. Rev. Lett. **72**, 2648 (1994)
5. S. Schuppler, S.L. Friedman, M.A. Marcus, D.L. Adler, Y.H. Xie, F.M. Ross, Y.L. Cha-bal, T.D. Harris, L.E. Brus, W.L. Brown, E.E. Chaban, P.F. Szajowski, S.B. Christman, P.H. Citrin, Phys. Rev. B **52**, 4910 (1995)
6. C.S. Garoufalis, A.D. Zdetsis, S. Grimme, Phys. Rev. Lett. **87**, 276402 (2001)
7. E. Degoli, G. Cantele, E. Luppi, R. Magri, D. Ninno, O. Bisi, S. Ossicini, Phys. Rev. B **69**, 155411 (2004)
8. I. Vasiliev, J.R. Chelikowsky, R.M. Martin, Phys. Rev. B **65**, 121302 (2002)
9. A. Puzder, A.J. Williamson, J.C. Grossman, G. Galli, J. Am. Chem. Soc. **125**, 2786 (2003)
10. A. Puzder, A.J. Williamson, J.C. Grossman, G. Galli, J. Chem. Phys. **117**, 6721 (2002)
11. Z. Zhou, L. Brus, R. Friesner, Nano Lett. **3**, 163 (2003)
12. M. Luppi, S. Ossicini, J. Appl. Phys. **94**, 2130 (2003)
13. Z. Zhou, R.A. Friesner, L. Brus, J. Am. Chem. Soc. **125**, 15599 (2003)
14. A.D. Zdetsis, C.S. Garoufalis, S. Grimme, NATO Advanced Research Workshop on "Quantum Dots: Fundamentals, Applications, and Frontiers" (Crete 2003) (Kluwer-Springer, 2005) pp. 317–332
15. C.S. Garoufalis, A.D. Zdetsis, Phys. Chem. Chem. Phys. **8**, 808 (2006)
16. A.D. Zdetsis, Rev. Adv. Mater. Sci.(RAMS) **11**, 56–78 (2006)
17. O. Akcakir, J. Therrien, G. Belomoin, N. Barry, J.D. Muller, E. Gratton, M. Nayfeh, Appl. Phys. Lett. **76**, 1857 (2000)
18. L. Mitas, J. Therrien, R. Twesten, M. Belomoin, G. Nayfeh, Appl. Phys. Lett. **78**, 1918 (2001)
19. S. Rao, J. Sutin, R. Clegg, E. Gratton, M.H. Nayfeh, S. Habbal, A. Tsolakidis, R. Martin, Phys. Rev. B **69**, 205319 (2004)

20. M.E. Casida in *Recent Advances in Density Functional Methods*, vol 1, ed. by D.P. Chong (World Scientific, Singapore, 1995)
21. P.J. Stephens, F.J. Devlin, C.F. Chabalowski, M.J. Frisch, J. Phys. Chem. **98**, 11623 (1994)
22. A.D. Becke, Phys. Rev. A **38**, 3098 (1988)
23. J.P. Perdew, Phys. Rev. B **33**, 8822 (1986)
24. R.B. Murphy, R.P. Messmer, Chem. Phys. Lett. **183**, 443 (1991)
25. R.B. Murphy, R.P. Messmer, J. Chem. Phys. **97**, 4170 (1992)
26. TURBOMOLE (Vers. 5.3), Universitat Karlsruhe (2000)
27. A. Schafer, H. Horn, R. Ahlrichs, J. Chem. Phys. **97**, 2571 (1992)
28. R. Bauernschmitt, R. Ahlrichs, Chem. Phys. Lett. **256**, 454 (1996)
29. S. Grimme, M. Waletzke, Phys. Chem. Chem. Phys. **2**, 2075 (2000)
30. M.J. Frisch et al., *Gaussian 03, Revision C.02* (Gaussian, Inc., Wallingford CT, 2004)
31. D. Sundholm, Phys. Chem. Chem. Phys. **6**, 2044 (2004)